FUNCTIONAL CME

Diffusion Tensor Imaging Tractography Tutorial and Introduction to Major White Matter Tract Anatomy and Function

T.A. Hijaz, E.N. McComb, S. Badhe, B.P. Liu, and A.W. Korutz

CME Credit

The American Society of Neuroradiology (ASNR) is accredited by the Accreditation Council for Continuing Medical Education (ACCME) to provide continuing medical education for physicians. The ASNR designates this enduring material for a maximum of 1 *AMA PRA Category 1 Credit*™. Physicians should claim only the credit commensurate with the extent of their participation in the activity. To obtain Self-Assessment CME (SA-CME) credit for this activity, an online quiz must be successfully completed and submitted. ASNR members may access this quiz at no charge by logging on to eCME at http://members.asnr.org. Nonmembers may pay a small fee to access the quiz and obtain credit via https://members.asnr.org/webcast/content/course_list.asp?srcNeurographics. Activity Release Date: January 2019. Activity Termination Date: January 2022.

ABSTRACT

DTI is frequently acquired in clinical practice during the preoperative evaluation and clinical work-up of patients; however, many radiology practices still do not routinely provide post-processed 3-dimensional images of the white matter tracts to the clinical services that ordered these studies. With standardized imaging and postprocessing techniques and a basic understanding of white matter anatomy, tractography can be performed quickly and reliably in clinical practice, often using postprocessing software that is already available for use by the radiologist. This article outlined the DTI protocol used at our institution, discussed the preferred locations of ROIs, addressed the optimal tractography parameters, and detailed the anatomy and function of the major white matter tracts.

Learning Objectives: 1) To describe the general physics principles behind DTI; 2) describe the proper locations for ROI placement when performing tractography of the major white matter tracts; 3) name white matter tracts based on shape, configuration, and position in the brain; and 4) describe functions of each of the major white matter tracts.

INTRODUCTION

DTI is an advanced MR imaging technique that has become valuable in a variety of clinical scenarios, including in patients with brain tumors, epilepsy, and traumatic brain injury. In patients with brain tumors, tractography is often performed before surgical intervention to evaluate the relationship between the important white matter tracts and the lesion. The possible effects of tumor on the white matter tracts include distortion from mass effect, infiltration, disruption, or reorganization. DTI has also been used to differentiate tumor infiltration from edema in the peritumoral region as well as help distinguish primary from metastatic brain tumors.[1,2]

DTI is also commonly used in localization and presurgical planning in patients with epilepsy. Specifically, DTI can be useful for defining the location of the Meyer loop of the optic radiations in temporal lobe epilepsy, which has variable anterior extension into the temporal region.[2,3] DTI

ABBREVIATION KEY

AF = arcuate fasciculus
CST = corticospinal tract
DSI = diffusion spectrum imaging
FA = fractional anisotropy
IFOF = inferior fronto-occipital fasciculus
ILF = inferior longitudinal fasciculus
SLF = superior longitudinal fasciculus
UF = uncinate fasciculus

Received September 1, 2017; accepted July 18, 2018.

From the Department of Radiology, Northwestern University Feinberg School of Medicine, Chicago, Illinois.

Please address correspondence to Alexander W. Korutz, MD, Department of Radiology, Northwestern University Feinberg School of Medicine, 676 N. St. Clair St. Suite 800, Chicago, IL 60611; e-mail: Alexander.Korutz@nm.org.

http://dx.doi.org/10.3174/ng.1700057

Disclosures
Based on information received from the authors, *Neurographics* has determined that there are no Financial Disclosures or Conflicts of Interest to report.

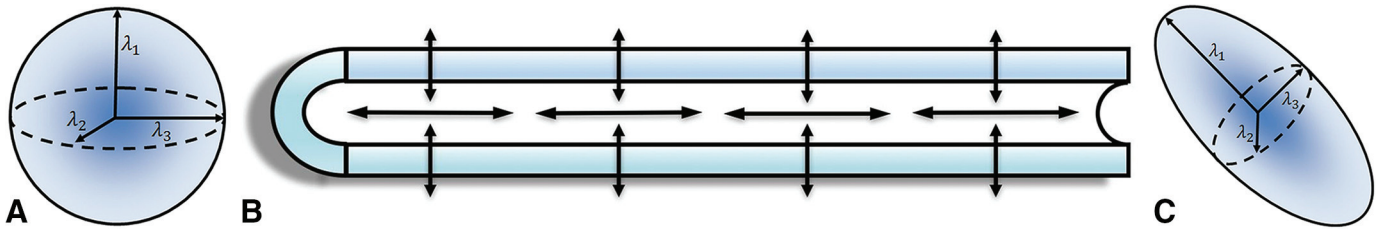

Fig 1. Isotropic versus anisotropic diffusion. *A*, Figure depicts a condition in which the likelihood of diffusion is equal in all directions (isotropic). *B*, Figure depicts that water is more likely to diffuse along the long axis of the axon (*long arrows*) rather than across its walls in the short axis (*short arrows*). *C*, Figure depicts a condition wherein the water is more likely to diffuse in one direction along λ_1 (anisotropic; *long arrow*).

$$\mathcal{D} = \begin{bmatrix} D_{xx} & D_{xy} & D_{xz} \\ D_{yx} & D_{yy} & D_{yz} \\ D_{zx} & D_{zy} & D_{zz} \end{bmatrix} \qquad \Lambda = \begin{bmatrix} \lambda_1 & 0 & 0 \\ 0 & \lambda_2 & 0 \\ 0 & 0 & \lambda_3 \end{bmatrix}$$

A **B**

Fig 2. Diffusion tensor matrix. *A*, Image depicts the standard 3 × 3 diffusion tensor matrix and the 6 unique directions that are contained in this 9-component matrix; it is for this reason that a minimum of 6 directions must be acquired to generate a DTI image. *B*, Image depicts the matrix that results after diagonalization, which yields 3 eigenvalues (λ_1, λ_2, and λ_3).

$$FA = \sqrt{\frac{3}{2}} \frac{\sqrt{(\lambda_1 - \bar{\lambda})^2 + (\lambda_2 - \bar{\lambda})^2 + (\lambda_3 - \bar{\lambda})^2}}{\sqrt{\lambda_1^2 + \lambda_2^2 + \lambda_3^2}}$$

$$where\ \bar{\lambda} = \frac{\lambda_1 + \lambda_2 + \lambda_3}{3}$$

Fig 3. FA calculation. Generation of an FA value can be performed with the knowledge of all 3 eigenvalues (λ_1, λ_2, and λ_3).

is also useful for localization of the seizure focus because white matter changes can be present adjacent to an epileptogenic cortical lesion. In traumatic brain injury, there can be microscopic disruption of the white matter, despite the lack of a macroscopic brain injury. In these settings, DTI has been useful for helping to diagnose the presence of traumatic brain injury as well as in guiding conversations about prognosis.[4] DTI has also been used to guide treatment for vascular lesions, particularly those located in the deep structures of the brain, and to localize ideal placement for deep brain stimulation.[2]

THEORY OF TRACTOGRAPHY

DTI is an MR imaging technique that uses direction-specific diffusion sensitizing gradients to generate images based on the random, thermally driven motion of water molecules in vivo. When there are no barriers to diffusion and the probability of diffusion is equal in all directions, the probability of diffusion can be represented as a sphere and can be described as isotropic (Fig 1*A*). However, when barriers to diffusion exist, such as those created by the cell membranes of axons, diffusion of water is more likely to occur along the long axis of the axon (Fig 1*B*). In this scenario, the probability of diffusion can be represented with an ellipse and can be described as anisotropic (Fig 1*C*). In either instance, the probability of diffusion in 3 dimensions can be represented mathematically using a 3 × 3 matrix. This 3 × 3 diffusion tensor matrix contains 6 unique values that constitute the minimum number of diffusion-encoded measurements (directions) that must be acquired in vivo with MR imaging to determine directionality (Fig 2*A*). In this matrix, subscripts are used (eg, *xx* or *yy*) to denote the unique direction in 3-dimensional space that a particular value is representing. Additional directions may be obtained and yield the benefit of improved accuracy of the tensor measurement.[5-7]

Table 1: White matter fiber orientation and corresponding color representation

Left-right	Red
Superior-inferior	Blue
Anterior-posterior	Green

Diagonalization is a mathematical process that can be applied to the 3 × 3 matrix to generate 3 orthogonal eigenvectors (ε_1, ε_2, and ε_3) whose respective magnitudes are represented by eigenvalues (λ_1, λ_2, and λ_3) (Fig 2*B*). These vectors represent the 3 orthogonal axes for an ellipsoid, which depicts the likelihood of water diffusion in 3 dimensions in the voxel being modeled. By convention, the direction of principle diffusion is represented by the largest of the eigenvalues and is denoted by λ_1. The second and third largest eigenvalues, λ_2 and λ_3, respectively, denote the rate of diffusion orthogonal to the direction of principle diffusion. An average of these 2 values will generate the parameter "radial diffusivity."

Alternatively, all 3 eigenvalues can be averaged to yield the "mean diffusivity," which denotes the diffusivity of water within a voxel that has been directionally averaged. The degree of anisotropy can be represented using fractional anisotropy (FA), which is represented by a number that ranges between 0 (completely isotropic) and 1 (maximally anisotropic), and is calculated from the 3 eigenvalues on a voxel-by-voxel basis (Fig 3). The direction of principle diffusion can be depicted on a color FA map using a red-green-blue color scale, with the FA value conveyed through color brightness (Table 1).[5-7] Color coding is typically standardized across scanner manufacturers.

Once generated, the color FA maps contain enough information on a voxel-by-voxel basis (principle direction of diffusion and FA magnitude) to allow for tractography to

extract information regarding white matter fiber orientation on a macroscopic scale. Deterministic tractography is currently the most commonly used method in the clinical setting. This method makes the assumption that fiber orientation is uniform throughout a voxel and only changes direction at the boundary with the adjacent voxel(s). In this technique, a user can place an ROI on a set of color FA images. This ROI serves as a seed point for the generation of 1 or more white matter tracts. Tract generation terminates when certain user-defined criteria are met, such as a minimum FA value or excessive turning angle. Additional ROIs may be placed and serve to restrict the output to only the tract(s) that pass through all ROIs. In contrast, probabilistic tractography is a more complex method that depicts a probability map (on a voxel-by-voxel basis) that a particular voxel is included on a path that connects with a user-defined ROI. Minimum FA values are typically not specified with this technique because the technique itself is useful for performing tractography in low FA regions, for example, gray matter. An excessive turning angle, however, may be used as a criterion for stopping the propagation of a tract. With either of these techniques, many of the major white matter tracts in the brain can be generated in a reliable fashion.[7]

Although concordance between tractography acquired from DTI and intraoperative direct subcortical stimulation is reported to be high, one should keep in mind some of the limitations of the former to avoid too heavy a reliance on the information obtained and generated by these techniques alone. One of the most frequently cited of these limitations is that the reproducibility and accuracy of these techniques are suboptimal due to the absence of a universally accepted, standardized analysis protocol. A related issue is that the tractography is very user-dependent, in part due to the discretionary nature of selection of FA thresholds.[8]

The major limitation of DTI occurs when white matter bundles with multiple different fiber orientations exist within a single imaged voxel. In this instance, the calculated FA value for a particular voxel will effectively be a weighted average of all of the fibers that are present within that voxel. This becomes problematic when trying to perform DTI tractography on white matter tracts that extend through regions that contain substantial crossing fibers. For instance, this is often evident when attempting to generate the corticospinal tract (CST). Although the dominant bulk of the fiber tract that extends from the region of the hand knob in the paramedian perirolandic region through the internal capsule and into the cerebral peduncle and brain stem is easily generated with an ROI-based approach, the fibers that extend laterally toward the representation of the face and tongue within the lateral perirolandic cortex are often truncated. This occurs due to the positioning of the arcuate fasciculus (AF) and superior longitudinal fasciculus (SLF) just lateral to the CST within the centrum semiovale.[6]

High angular resolution DWI and diffusion spectrum imaging (DSI) are 2 imaging techniques that attempt to combat some of the limitations of DTI and yield more accurate information with regard to white matter fiber orientation, though each requires a longer acquisition time than DTI and more complex postprocessing. Technical advancements, including the use of multiple receiver coils, simultaneous multislice echoplanar imaging, and multiband excitation, have sufficiently decreased acquisition times to allow the clinical use of DSI.[8]

Diffusion kurtosis imaging, which has a shorter scan time than DSI, is another technique that has shown potential to be superior to traditional DTI.[8] DWI and DTI are based on a Gaussian distribution of water molecules, familiar to most people as a bell curve distribution. In vivo diffusion of water molecules is far more complex than this model implies. Kurtosis is a term from probability theory and statistics that refers to deviation from a normative distribution. Diffusion kurtosis imaging attempts to account for the non-Gaussian characteristics of water diffusion in the brain.[9]

In the setting of tumor, distortion of the anatomy, including the white matter structure, may cause DTI to underestimate the amount of remaining functional white matter. There also is the related issue of brain shift during surgery, which results in a loss of congruence between the intraoperative findings and the preoperative imaging. To account for this, several investigators have recommended using a "buffer" of at least 5–10 mm when operating in proximity to eloquent structures. The current consensus is that the neurosurgeon best minimizes the risk of unintended injury to the patient by relying on a combination of imaging-based navigational information and intraoperative subcortical mapping.[8]

After briefly reviewing the fundamental principles of DTI and tractography and some of the limitations thereof, herein, we outlined the DTI protocol used at our institution, discussed the preferred ROI locations and tractography parameters, and detailed the anatomy and function of the major white matter tracts, including the CST, inferior fronto-occipital fasciculus (IFOF), AF and SLF, optic radiations, uncinate fasciculus (UF), inferior longitudinal fasciculus (ILF), and the cingulum.

IMAGING TECHNIQUE

Scan Parameters

DTI examinations at our institution are obtained on a 3 Tesla system (Verio or Skyra, Siemens Medical Systems, Erlangen, Germany) using a 12-channel head coil with the following pulse sequence parameters: TR/TE/excitations, 10700 ms/83 ms/4; EPI factor, 104; 230-mm field of view; 2-mm sections; 54 sections; matrix, 116 × 116; voxel size, 2 × 2 × 2 mm; bandwidth, 1596 Hz/Px; echospacing, 0.71 ms; and diffusion encoding in 64 directions. Typically, the acquisition time is 10–11 minutes per scan using the aforementioned parameters. DTI postprocessing and tractography are performed with either Prism (Prism Clinical

Imaging, Elm Grove, Wisconsin) or BrainLab software (BrainLab, Munich, Germany).

ROI Selection

The reproducibility of tractography is difficult to distill into a simple statement because it depends on a variety of factors, including the imaging parameters that were used, the particular tract being interrogated, and the tracking algorithm used. Accurate fiber tracking, though difficult to achieve at times, can be optimized by reconstructing tracts whose courses have been well established through previous anatomic studies. Even when results are reproducible, it is important to remember that there is always some variability in reconstruction that arises from data acquisition issues, such as patient motion and partial volume effects. Wakana et al[10] approached the problem of generating reproducible tracking protocols by separating it into 2 steps; the first was to find out which tracts could be reconstructed with consistent results, which depended on the size, curvature, and discreteness of the tract in question, while the second was to refine the protocols used to reconstruct the tracts through iterations of the protocol setup and measurements of reproducibility.[10]

With the aforementioned issues of reproducibility in mind, a systematic approach is recommended when performing ROI-based DTI tractography in clinical practice. At our institution, this is typically performed after the placement of two 3-dimensional cubic ROIs in the regions of the brain where the tract of interest is the only major white matter bundle that passes through both points.

For the CST, the first ROI is placed over the sensorimotor region for the foot, fingers, lip, and tongue areas. A second ROI can be placed either over the ventral aspect of the cerebral peduncles or the posterior limb of the internal capsule, depending on user preference. For the AF, the first ROI is placed within the lateral aspect of the centrum semiovale over the anteroposterior (represented in green) portion of the dorsal limb of the AF. The second ROI can be placed over the superior-inferior (represented in blue) portion of the tract, which connects the dorsal and ventral limbs. For the IFOF, large ROIs are placed overlying the anterior and posterior portions of the tract within the anterior frontal and occipital lobes, respectively. For the optic radiations, the first ROI is placed over the lateral geniculate nucleus of the thalamus, and the second ROI can be placed over the cortex along the calcarine fissure within the occipital lobe. The lower bank may be specifically selected to target the fibers of the optic radiations that contribute to the Meyer loop. For the ILF, the first ROI is placed over the anterior temporal lobe, whereas the second ROI is placed overlying the ipsilateral occipital lobe. For the UF, ROIs are placed overlying the anterior–inferior frontal lobe as well as the ipsilateral anteromedial temporal lobe. For the cingulum, a single ROI can be placed over the dominant anteroposterior-oriented component of the tract, which is located just above the body of the corpus callosum.

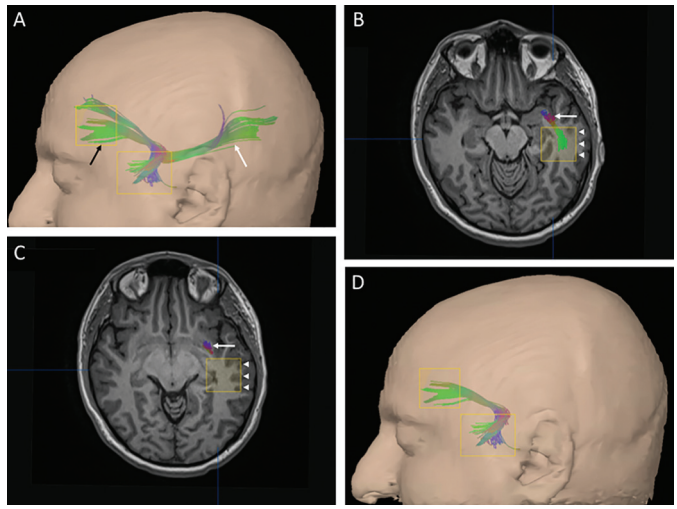

Fig 4. Exclusion of spurious fibers. *A*, A volume-rendered image that demonstrates ROIs within the anterior–inferior frontal lobe as well as the anterior temporal lobe; tractography performed with these ROIs returned the desired tract, the UF (*black arrow*), in addition to other spurious fibers, some of which include the IFOF (*white arrow*). *B* and *C*, Axial MPRAGE images with overlaid tracts; the *white arrow* in both images depicts the desired tract, the UF; the *white arrowheads* in both images depict a manually placed ROI before and after the exclusion of unwanted fibers *B* and *C*, respectively. *D*, Depicts a volume-rendered image that demonstrates the final result, the UF.

In all instances, additional ROIs may be placed after the generation of a tract to exclude unwanted and/or spurious fibers. In Figure 4, ROIs in the anterior–inferior frontal lobe and anterior temporal lobe successfully generated the UF in addition to spurious fibers, some of which represent the IFOF. These spurious fibers were excluded by selecting them with a third ROI and using the postprocessing software functionality to erase them. When determining whether a specific tract is accurate or whether the tract contains erroneously generated fibers or fibers from an adjacent tract(s), it is important to have a working knowledge of normal white matter anatomy.

In addition, we also find it helpful when the process of tractography can be guided by information that is present on other advanced imaging sequences that are typically acquired along with DTI. For instance, the location and course of the AF can often be inferred from cortical activity that is seen in the temporal, parietal, and frontal lobes with many task-based functional MR imaging language paradigms. An example of this concept is presented in Figure 5. In this figure, short fibers can be seen connecting activation blobs in the frontal, parietal, and posterior temporal lobes with the dominant bulk of the AF. In this scenario, identification of a fiber tract as the AF could be aided by this finding.

DTI Parameters

In addition to ROI selection when performing DTI tractography, many software platforms also allow the user to adjust other parameters during the tractography process. Some of these parameters include fiber length, minimum FA value, and fiber turning angle. In the case of fiber tract

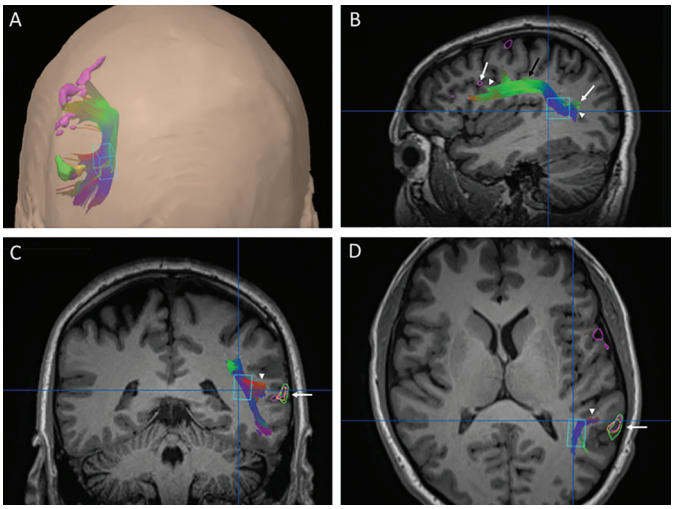

Fig 5. Blood oxygen level-dependent (BOLD) fMRI guiding tractography. *A*, A volume-rendered image that contains language activation blobs as derived from multiple task-based fMRI language paradigms as well as the AF. *B*, *C*, and *D*, Sagittal, coronal, and axial MPRAGE images, respectively, with the same activation blobs and AF as depicted in (*A*). Please note the short AF fibers (*white arrowheads*) that connect the dominant fiber tract bundle (*black arrow* in *B*) with the adjacent activation blobs (*white arrows*).

Table 2: Suggested DTI tractography starting parameters

	FA	Length (mm)	Angle (degrees)
AF and SLF	0.15–0.25	50–60	60
Cingulum	0.15–0.20	30	60
CST	0.20–0.25	70–80	60
IFOF	0.15–0.25	70–80	60
ILF	0.20–0.25	50	40–50
Optic radiations	0.15–0.25	40	60
UF	0.15–0.25	20–30	30

length, this parameter serves to eliminate fiber tracts that are shorter than the tract that is being targeted. It is for this reason that we choose a longer length (eg, 75 mm) for longer tracts such as the CST and IFOF. Minimum FA value is a parameter that provides an FA floor below which a tract will not propagate. In practice, we believe that FA values between 0.25 and 0.30 are ideal starting values; however, it is often necessary to reduce this value (0.15–0.25) to generate a desired tract, particularly when targeting tracts that are in close proximity to a pathologic process. Generally, FA values <0.15 generate spurious fibers, which should be scrutinized closely before accepting as accurate. Finally, turning angle is a parameter that attempts to prevent the generation of tracts that take "nonphysiologic" angles (eg, >90°). In general, a turning angle between 40° and 70° is often appropriate. Although definitive starting FA, turning angle, and tract length values are impossible to enumerate for each tract covered in this article, general guidelines for starting values are listed in Table 2. These values are based on a review of the literature as well as our own clinical experience.[11-17]

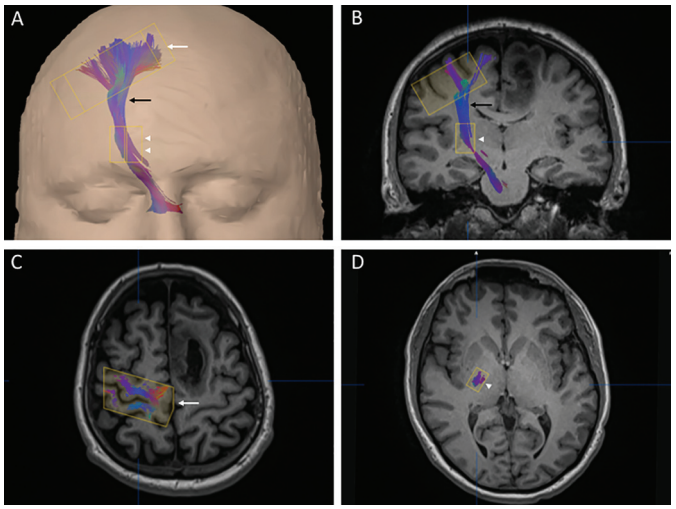

Fig 6. CST. Volume-rendered image (*A*) as well as coronal (*B*) and axial (*C*, *D*) MPRAGE images that demonstrate the CST (*black arrows*) in addition to 2 ROIs: the first is placed over the sensorimotor cortex (*white arrows*) and the second is placed over the posterior limb of the internal capsule (*white arrowheads*).

ANALYSIS OF MAJOR DIFFUSION TRACTS

CST

White matter tracts are divided into association fibers (which connect different ipsilateral cortical regions), commissural fibers (which connect the hemispheres across the midline), and projection fibers (which connect the cortex with deep gray matter, the brain stem, and the spinal cord). The CST is a projection tract that originates in the primary motor cortex, the primary somatosensory cortex, the supplementary motor area, and the premotor cortex (Fig 6).[5,18-20] A recent study showed that nearly 70% of CST fibers originate from the primary motor and somatosensory cortices, 20% arise from the supplementary motor area, and 10% arise from the dorsal premotor cortex.[19] Additional projections arise from the posterior parietal cortex, parietal operculum, and cingulate gyrus.[18,21,22]

The fibers of the CST then run through the centrum semiovale and corona radiata to the posterior limb of the internal capsule and the cerebral peduncle, at which point the CST is located within the middle third of the crus cerebri. The CST fibers traverse the basis pontis, enter the ventral medulla, forming the medullary pyramids. At the level of the caudal medulla, near the cervicomedullary junction, most of the CST (75%–90%) decussates and crosses into the contralateral spinal cord to form the lateral CST.[18,20] These fibers synapse on the anterior horn cells at their respective spinal levels. The remaining CST fibers descend into the ipsilateral spinal cord and form the anterior CST (approximately half of the uncrossed fibers) and also join contralateral crossed fibers within the lateral CST (remaining fibers). These fibers remain ipsilateral to the side of origin and do not cross to the contralateral anterior horn cells until they reach their designated spinal level.[18,20] Of note, the corticobulbar and corticopontine tracts travel

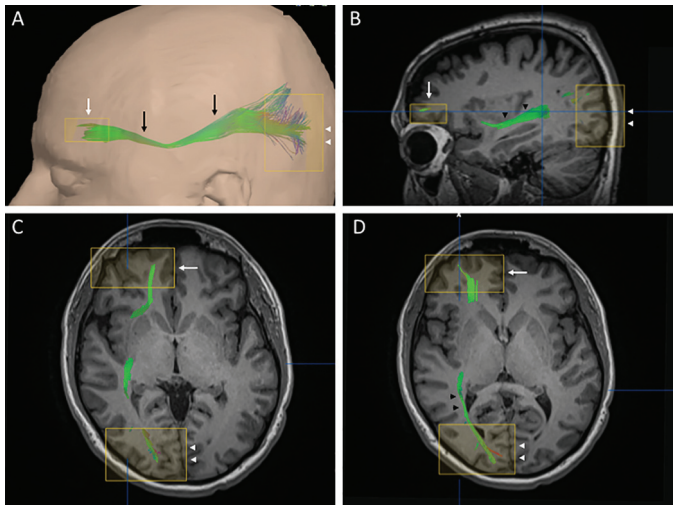

Fig 7. IFOF. Volume-rendered image (*A*) as well as sagittal (*B*) and axial (*C* and *D*) MPRAGE images, demonstrating the IFOF (*black arrows*) in addition to 2 ROIs: the first is placed over the anterior-inferior frontal lobe (*white arrows*), and the second is placed over the occipital lobe (*white arrowheads*). *B*, The *black arrowheads* depict the IFOF as it courses through the inferior aspect of the external capsule. The *black arrowheads* in (*D*) depict the IFOF within the sagittal stratum.

with the CST to the level of the brain stem, but it is difficult to distinguish these tracts on DTI.

The CST has somatotopic organization similar to the primary motor and somatosensory cortices. In both the corona radiata and posterior limb of the internal capsule, the anterior fibers represent the face, the middle fibers represent the arm, and the posterior fibers represent the leg.[23,24] Within the cerebral peduncle, there is an oblique orientation with the anteromedial fibers representing the face, the middle fibers representing the arm, and the posterolateral fibers representing the leg.[18,25] The fibers for the arm and hand remain anteromedial and medial to the fibers for the leg and foot in the pons and medulla, respectively.[18,26-28] The fibers that represent the face (corticobulbar) project to the cranial nerve nuclei in the brain stem.

The CST is considered to be a multifunctional white matter tract that has roles in movement execution (primary motor cortex), visual and sensory direction for movement (premotor cortex), design and coordination of movement (supplementary motor area), management of afferent sensory input related to movement (somatosensory cortex), and, potentially, an emotional component of movement (cingulate cortex).[29,30] With regard to the execution of movement, it is thought that the lateral CST controls distal, fine motor skills, whereas the anterior CST regulates proximal movement of the upper extremities, the body, and the trunk.[29,31]

IFOF

The IFOF is an association fiber tract that connects the occipital, posterior parietal, temporal, and frontal lobes (Fig 7). Posteriorly, the IFOF extends from the cortex through the sagittal stratum, which is located in the white matter lateral to the posterior horn and atrium of the lateral ventricle. The sagittal stratum is formed by the IFOF, the ILF, a portion of the AF and SLF, and a portion of the optic radiations.[5,20,32] After traversing the sagittal stratum, the tract extends along the inferolateral margin of the claustrum and joins the external and extreme capsules. In this area, it is located superior to the UF within the temporal stem. The fibers then project into various locations in the frontal lobe. Of note, the posterior portion of the IFOF is parallel to the ILF, and these 2 tracts can be difficult to differentiate in the occipital region on DTI.

The IFOF is composed of a superficial layer, a dorsal layer, and a deep, ventral layer.[33-37] The superficial layer connects the extrastriate cortex of the occipital lobe (superior and middle occipital gyri), the superior parietal lobule, and the superior temporal gyrus to the inferior frontal gyrus. The deep layer can be subdivided into 3 parts: posterior, middle, and anterior. The deep layer connects the inferior occipital gyrus, the inferior temporo-occipital region, and the middle temporal gyrus to the 1) middle frontal gyrus and dorsolateral prefrontal cortex (posterior fibers), 2) middle frontal gyrus and lateral orbitofrontal gyrus (middle fibers), and 3) basal orbitofrontal cortex (anterior fibers).

In 2016, Wu et al[38] published the results of their work to further define the anatomy of the IFOF using a higher-resolution DSI technique. Specifically, they used an attenuated sampling of angular space and reconstructed the tractography using generalized q-sampling imaging with a high angular resolution-based approach.[38] Although many standard descriptions of the IFOF have described 2 major segments, the approach taken by Wu et al[38] helped reveal 5 constituent components of this tract. The investigators also found a fair amount of variability among individuals with regard to connectivity of the IFOF, with the highest degree of overlap (40%) in the central portion of the tract.[38]

One of the roles of the IFOF is to function as part of the ventral language stream. The current concept of language processing is a dual-stream model composed of ventral and dorsal streams. The ventral stream is predominantly bilateral and involved in semantic processing (verbal and nonverbal), speech recognition, and lexical processing. The dorsal stream is often strongly lateralized to the left hemisphere and involved in phonologic processing as well as auditory-motor integration.[39-41] The major white matter tracts associated with the ventral language stream are the IFOF, the ILF, the UF, and the middle longitudinal fasciculus. It has been proposed that these white matter tracts comprise both direct and indirect pathways for the ventral language stream.[35,37,42]

The direct pathway is represented by the IFOF and is considered to be essential because the other white matter tracts do not compensate for IFOF deficits. The indirect pathway is via the ILF and the UF. Deficits of the indirect pathway have been compensated for by the IFOF, which supports the idea of plasticity. The different layers of the

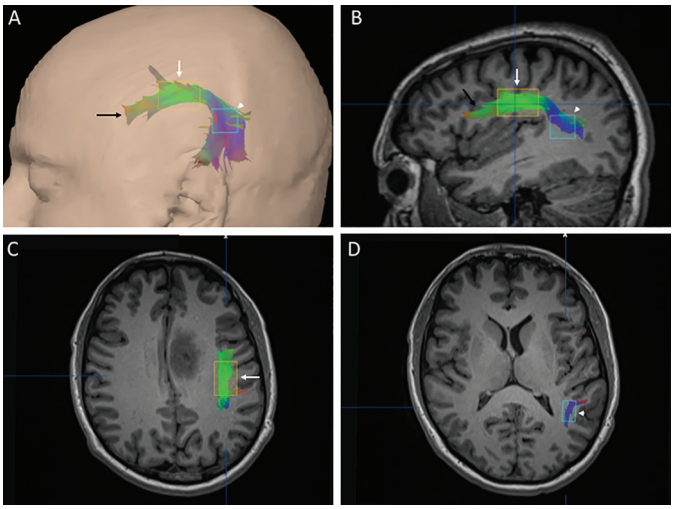

Fig 8. AF and SLF. Volume-rendered image (*A*) and sagittal (*B*) and axial (*C*, *D*) MPRAGE images, demonstrating the AF and SLF (*black arrows*) in addition to 2 ROIs, the first of which is placed in the lateral aspect of the centrum semiovale over the anteroposterior portion of the dorsal limb of the AF and SLF (*white arrows*), and the second of which is placed over the superior-inferior portion of the tract that connects the dorsal and ventral limbs (*white arrowheads*).

IFOF are suggested to support different functions.[34,35,37,43] For example, the superficial layer and the posterior fibers of the deep layer likely represent semantic processing, whereas the middle fibers of the deep layer function in sensory-motor integration, and the anterior fibers of the deep layer may have a role in the emotion-speech interface.

Another important function of the IFOF involves the ventral visual stream. There is a dual-stream model for vision, with a ventral visual stream that is responsible for object recognition and a dorsal visual stream that recognizes spatial relationships and guides movement.[44-47] The ventral pathway involves the occipitotemporal cortex, inferior parietal lobule, and dorsolateral prefrontal cortex. The major white matter tracts associated with the ventral visual stream are the IFOF, ILF, and the UF. These tracts are thought to be involved in ventral stream functions, such as face recognition, color processing, object identification, and text semantics as well as visual memory, visual emotion, reading, and attention.[44,48-51] Given the role of the IFOF in many high-order functions, it is of interest that the IFOF has no equivalent tract in the monkey brain, which led some investigators to believe that this unique human tract may be necessary for the development of higher cognitive skills.[35,52,53]

AF and SLF

The AF and SLF are association fiber tracts that connect the temporal, parietal, and occipital lobes to the frontal lobe via an arc around the sylvian fissure (Fig 8). Earlier literature considered these tracts to be part of the same fasciculus, and the terms have been used interchangeably. More recent work has defined these tracts as being more distinct from one another. Many recent models consider the SLF to be subdivided into 4 separate components: the SLF-I, SLF-II, SLF-III, and AF.[18,20,37,43,54,55] That said, it is important to note that there is no universal agreement on the subcomponents of the SLF. This controversy likely results in part from continued refinements of tractography techniques, such as the improved resolution afforded by the more recent use of DSI compared with earlier studies based on DTI. In their study of the SLF, Wang et al[56] noted that, even when the same imaging technique (eg, DSI) is used, there is variation in the subcomponents of the tract among healthy individuals. Furthermore, there are differences in these tracts between the 2 cerebral hemispheres.[56]

As noted above, the initial model of the AF and SLF that connects the Wernicke area (superior temporal cortex) to the Broca area (inferior frontal cortex) is too simplistic. The recent models of the SLF have determined a specific course for each of its subcomponents. The SLF-I connects the superior parietal lobe–precuneus with the supplementary motor area, premotor areas, and, likely, the anterior cingulate region. The SLF-II connects the inferior parietal lobe–parieto-occipital region with the angular gyrus and middle frontal gyrus. The SLF-III connects the supramarginal gyrus with the pars opercularis of the inferior frontal gyrus. The AF connects the superior and middle temporal gyri with fronto-opercular locations.

Results of several studies have indicated that the AF is composed of different components, including a recent study that identified ventral and dorsal segments of the AF.[55] The ventral AF segment coursed deep to the supramarginal gyrus and continued with the SLF-III to the pars opercularis as well as the pars triangularis and ventral premotor cortex, and the dorsal AF segment coursed deep to the angular gyrus and continued with the SLF-II to the middle frontal gyrus as well as the pars opercularis and ventral premotor cortex.[55] However, it should be noted that there is variability in the descriptions of the subcomponents of the AF among different investigators.

The AF and SLF are the major white matter tracts of the dorsal language stream but also have roles in the dorsal visual stream. As noted above, the dorsal language stream is involved in phonologic processing as well as auditory-motor integration and is often left-hemisphere dominant.[39-41] The dorsal visual stream recognizes spatial relationships and guides movement. The functions of the AF and SLF can vary, depending on whether they are located in the dominant or nondominant hemisphere. In the dominant hemisphere, the SLF-III and AF have roles in the articulation of speech, phonologic processing, and lexical semantics, whereas, in the nondominant hemisphere, the SLF-III and AF have roles in visuospatial attention and prosody of language.[48,55,57,58]

The bilateral SLF-I and SLF-II fibers have similar functions in both the dominant and nondominant hemispheres. The SLF-I is thought to help regulate higher motor function, whereas the SLF-II has roles in spatial working memory and visual spatial awareness. It is interesting to note that comparative studies between humans and lower primates have

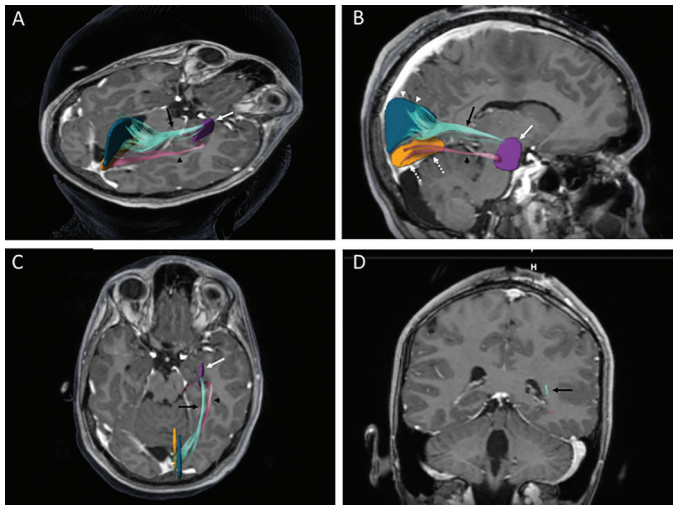

Fig 9. Optic radiations. Volume-rendered image (*A*) and sagittal oblique (*B*), axial (*C*), and coronal (*D*) MPRAGE images, demonstrating the optic radiations Baum loop (*black arrows*) and Meyer loop (*black arrowheads*). Both loops can be generated by placing an ROI within the lateral geniculate nucleus of the thalamus (*white arrows*). The Baum loop can be generated by placing a second ROI over the cortex along the superior aspect of the calcarine fissure (*white arrowheads*). The Meyer loop can be generated by placing a second ROI over the cortex along the inferior aspect of the calcarine fissure (*white dashed arrows*).

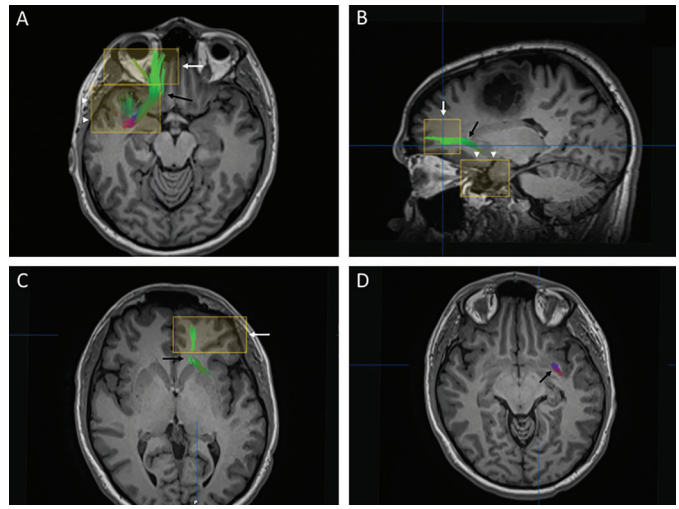

Fig 10. UF. *A*, The entire volume-rendered UF (*black arrow*) overlaid on a single axial MPRAGE image. *B–D*, Sagittal (*B*) and axial (*C* and *D*) MPRAGE images with the appropriate portion of the UF (*black arrows*) overlaid on each image. Two ROIs are depicted in *A–C*: the first is located in the anterior-inferior frontal lobe (*white arrows*), and the second is located in the temporal lobe (*white arrowheads*). The *black arrow* in *D* depicts the UF as it travels through the anterior-inferior aspect of the external capsule.

shown a difference in the connections between the left frontal cortex and the left middle and inferior temporal gyri.[59,60] Although these connections are robust in humans, they are either diminutive or absent in the lower primates, which suggests that the connections support the higher cognitive and language functions in humans.[59,60]

Optic Radiations

The visual pathway begins at the eyes and extends along the optic nerves to the optic chiasm and optic tracts. The optic radiation, which is the posterior portion of the visual pathway, is composed of fibers that originate from the posterior dorsolateral portion of the lateral geniculate nucleus, the structure into which fibers from the ipsilateral optic tract course (Fig 9). A smaller, ventral fiber bundle, known as the Meyer loop, initially travels anteriorly and laterally, and then turns sharply posteriorly and medially around the temporal horn of the lateral ventricle, ultimately terminating in the inferior calcarine cortex of the occipital lobe. A larger, dorsal fiber bundle (Baum loop) departs the lateral geniculate nucleus and becomes more compact, briefly coursing laterally and then turning posteriorly and medially to terminate in the upper calcarine cortex.[61] Additional visual input fibers travel from either the lateral geniculate nucleus or the pulvinar nucleus of the thalamus to areas of motion-specialized cortex along the lateral aspect of the occipital lobe.[61] The optic radiation, along with the ILF, IFOF, and a portion of the AF and SLF, is considered to be a component of the sagittal stratum, which is situated lateral to the atrium of the lateral ventricle.[62]

The optic radiation is one of the earliest white matter tracts to mature, and it is fully myelinated by 3 years of age.[63] One portion of the optic radiation is myelinated at birth and extends from the lateral geniculate nucleus to the calcarine cortex. The other group of fibers is myelinated postnatally, and these fibers course from the extracalcarine cortex to the pulvinar nucleus of the thalamus.[61]

From a functional standpoint, the role of the optic radiation is to relay visual impulses received in the lateral geniculate nucleus to the visual cortex of the occipital lobe. It is important to note that the visual pathway conserves retinotopic organization. The visual field on a particular side travels via the optic radiation of the opposite cerebral hemisphere to the visual cortex.[64] One setting in which preoperative visualization of the course of the optic radiation when using tractography can be helpful is epilepsy surgery. It has been noted that a large number of patients who underwent anterior temporal lobectomy for epilepsy were left with a visual field defect.[65]

UF

The UF, whose name is derived from the Latin word for "hook," which thus reflects its morphology, is a ventrally located association tract (Fig 10). It travels from the anterior portion of the temporal lobe to the orbitofrontal cortex. Its temporal fibers are located anterior and medial to the ILF. As the fibers of the UF pass through the anterior aspect of the external capsule, they are generally positioned slightly inferior to those of the IFOF.[32] Given the location of the UF, it is susceptible to injury in head trauma. It is also sometimes injured during epilepsy surgery.[66]

The UF does not reach its developmental peak until the third decade of life. Overall, the functions of the UF remain largely unknown, although, as part of the extended limbic system, this tract is involved in emotions and language.[66] In

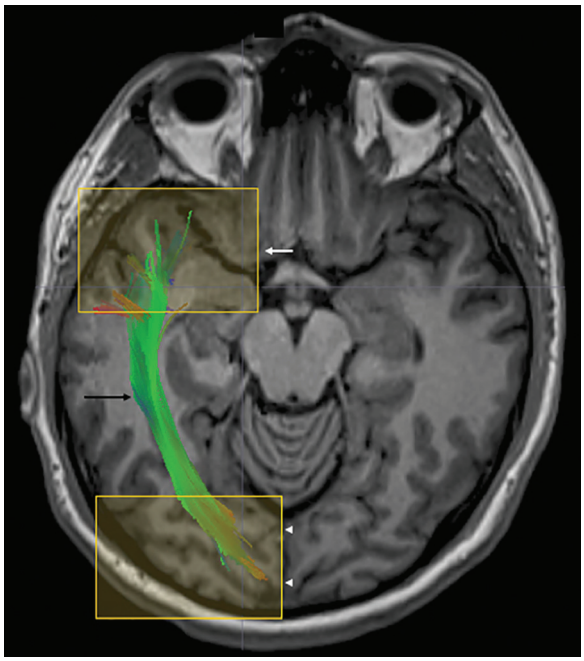

Fig 11. ILF. The entire ILF overlaid on a single axial MPRAGE image (*black arrow*). Two ROIs were used to generate this tract: the first located in the anterior temporal lobe (*white arrow*) and the second is located in the occipital lobe (*white arrowheads*).

addition, studies of patients with lesions that involved the UF also implicate it in the formation and retrieval of episodic memories.[67-70] As described previously, the UF is a component of both the ventral language and ventral visual streams. The ventral language stream contains both direct (IFOF) and indirect (ILF and UF) pathways and is involved in semantic processing of verbal and nonverbal language.[37,39-42,71] The ventral visual stream is also composed of both direct (IFOF) and indirect (ILF and UF) pathways, with the ventral stream performing tasks related to object recognition.[44-47] The UF has been implicated in various developmental and psychiatric disorders.[66] Despite its relatively short course, it is clear that the UF plays a role in many higher-level cognitive processes.

ILF

The ILF, which is part of the lateral group of long association fibers, courses laterally and inferiorly cephalad to the optic radiation and connects the anterior temporal lobe with the occipital lobe (Fig 11).[72] The IFOF overlaps a portion of the course of the ILF.[73] In contrast to the IFOF, which is a direct pathway that joins the orbitofrontal, posterior temporal, and occipital portions of the hemisphere, the ILF is considered to be an indirect pathway. It connects similar portions of the hemisphere and, along with the UF, communicates with the orbitofrontal region.[74]

Direct and indirect subdivisions of the ILF have been described.[73] The indirect pathway is formed by U-shaped fibers that join adjacent gyri in the inferior temporal and occipital convexities. Longer fibers located medial to the aforementioned shorter fibers comprise the direct pathway, and they connect with the superior, middle, and inferior temporal gyri, fusiform and parahippocampal gyri, amygdala, and hippocampus.[32,49,73,75]

The direct pathway of the ILF has also been subdivided into dorsal and ventral components. The dorsal ILF is the more lateral component. The ventral ILF begins in the fusiform gyrus and travels along the inferolateral aspect of the lateral ventricle to the parahippocampal gyrus and inferior temporal pole. Research has also suggested the existence of a lingual cortex-to-amygdala bundle.[76] It is thought to originate from the medial aspect of the lingual cortex and course along the inferolateral wall of the lateral ventricle medial and deep to the ventral ILF. At the temporal horn, the lingual cortex-to-amygdala bundle of the ILF travels medially and terminates in the region of the amygdala.[76]

As with some of the other major white matter tracts, the functions of the ILF remain incompletely understood. That said, results of research have indicated a variety of possible roles for this major tract.[76] Together, the aforementioned dorsal ILF and ventral ILF connect areas of cortex activated by various visual inputs, regions involved in multimodal processing of stimuli (the lateral infero temporal multimodal area for language), and the anterior temporal pole, where the overlapped terminations of the ILF and UF create a communication with the direct pathway of the semantic ventral stream for language analysis (IFOF) and the dorsal visual stream involved in the analysis of the spatial position of visual cues. The lingual cortex-to-amygdala bundle of the ILF is thought to be involved in limbic modulation of visual processing.[76]

Ortibus et al[77] used DTI to assess for differences in the ILF of children with object recognition deficits compared with healthy individuals. They found an association between the loss of integrity of the ILF and impaired object recognition.[77] The ILF has also been implicated in the recognition of facial emotional expression.[78]

Some functions of the ILF seem to be lateralized. For example, results of research indicate that reduced FA in the right ILF negatively correlates with measures of thought disorders.[79] Reduced FA in several white matter tracts, including the left ILF, has been associated with impaired cognitive flexibility.[80] A study of adolescents with schizophrenia found evidence of reduced FA in the left ILF, particularly in patients who had experienced visual hallucinations.[15] Language function associated with the ILF also seems to be lateralized. Work by Mandonnet et al[81] indicates that the left ILF is one part of the indirect subdivision of the ventral semantic stream.

Cingulum

The cingulum, a portion of which runs superior and parallel to the corpus callosum, is a medially located association tract with a somewhat C-shaped configuration (Fig 12). Fibers of the cingulum travel from each temporal lobe, specifically from the amygdala, uncus, and parahippocampal gyrus, to the orbitofrontal portion of each frontal lobe in-

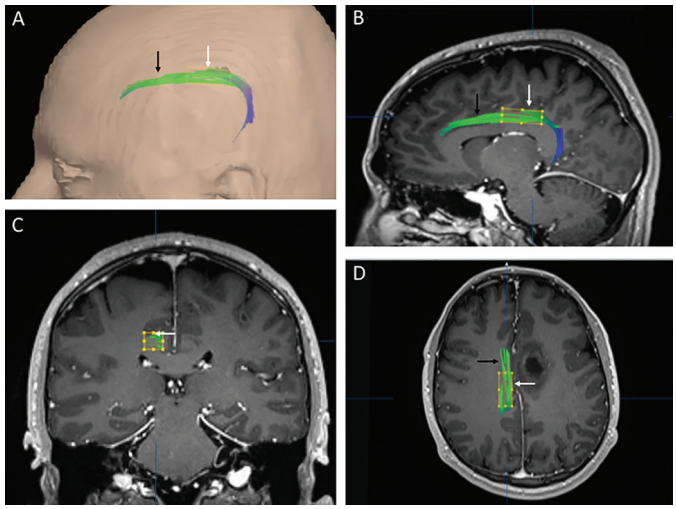

Fig 12. Cingulum. Volume-rendered image (*A*) and sagittal (*B*), coronal (*C*), and axial (*D*) MPRAGE images demonstrating the cingulum (*black arrows*), as generated by a single ROI placed in the dominant anteroposterior portion of the tract within the white matter of the cingulate gyrus (*white arrows*).

ferior to the callosal genu. In addition, there are shorter fibers traveling to and from the main structure of the cingulum and connecting to various other portions of the cerebral cortex, including each cingulate gyrus, each medial frontal gyrus and paracentral lobule, the precuneus of each parietal lobe, the cuneus and lingual gyrus of each occipital lobe, and each fusiform gyrus.[60]

Traditionally, the cingulum, a component of the limbic system, has been divided into anterior, middle, and posterior portions, which were initially defined by their cellular structure and receptor types. These partitions were later further defined by functional imaging and electrical stimulation.[82] The subdivisions of the cingulum also seem to have different functional roles. The anterior component is involved in decision-making, emotion, and executive function.[83,84] The middle section of the cingulum helps to carry out both motor function and attention-related tasks.[85] Cognitive function is found in the posterior portion.[86,87]

Recently, Wu et al[82] used DTI and fiber dissection to identify 5 component segments of the cingulum: segment I courses from the orbitofrontal cortex to the precuneus and splenium of the corpus callosum; segment II arises in the parahippocampal gyrus, travels around the splenium, and terminates in the medial portion of the superior frontal gyrus; segment III, the largest of the fiber bundles, originates in the superior parietal lobule and precuneus, and joins the medial aspect of the superior frontal gyrus; a smaller component, extending from the superior parietal lobule and precuneus to the supplementary and premotor areas of the frontal lobe, is designated segment IV; and segment V extends from the parahippocampal gyrus to the occipital lobe.

The function of segment I has not been determined fully, though results of studies indicate potential roles, including modulating affective responses to noxious stimuli and perhaps in depression, cognitive function, and verbal memory. Segment II is thought to perhaps play a role in path integration, which involves updating position and orientation. Given its multiple interconnections, there is speculation that, of the subdivisions of the cingulum, segment III may have the dominant functional role, and among its possible roles are performance in attention-intensive cognitive tasks and response conflict. Segment V may have multiple functions, including in cognition, executive function, and memory.[82]

CONCLUSIONS

When using these DTI and tractography techniques combined with basic knowledge of the anatomy and function of the white matter tracts themselves, a radiologist can effectively implement a well-rounded DTI program at his or her institution.

REFERENCES

1. Sternberg EJ, Lipton ML, Burns J. **Utility of diffusion tensor imaging in evaluation of the peritumoral region in patients with primary and metastatic brain tumors.** *AJNR Am J Neuroradiol* 2014;35:43–44. 10.3174/ajnr.A3702
2. Essayed WI, Zhang F, Unadkat P, et al. **White matter tractography for neurosurgical planning: a topography-based review of the current state of the art.** *Neuroimage Clin* 2017;15:659–72. 10.1016/j.nicl.2017.06.011
3. Yogarajah M, Focke NK, Bonelli S, et al. **Defining Meyer's loop-temporal lobe resections, visual field deficits and diffusion tensor tractography.** *Brain* 2009;132:1656–68. 10.1093/brain/awp114
4. Hulkower MB, Poliak DB, Rosenbaum SB, et al. **A decade of DTI in traumatic brain injury: 10 years and 100 articles later.** *AJNR Am J Neuroradiol* 2013;34:2064–74. 10.3174/ajnr.A3395
5. Jellison BJ, Field AS, Medow J, et al. **Diffusion tensor imaging of cerebral white matter: a pictorial review of physics, fiber tract anatomy, and tumor imaging patterns.** *AJNR Am J Neuroradiol* 2004;25:356–69
6. Alexander AL, Lee JE, Lazar M, et al. **Diffusion tensor imaging of the brain.** *Neurotherapeutics* 2007;4:316–29. 10.1016/j.nurt.2007.05.011
7. Nucifora PG, Verma R, Lee SK, et al. **Diffusion-tensor MR imaging and tractography: exploring brain microstructure and connectivity.** *Radiology* 2007;245:367–84. 10.1148/radiol.2452060445
8. Salama GR, Heier LA, Patel P, et al. **Diffusion weighted/tensor imaging, functional MRI and perfusion weighted imaging in glioblastoma-foundations and future.** *Front Neurol* 2017;8:660
9. Steven AJ, Zhuo J, Melhem ER. **Diffusion kurtosis imaging: an emerging technique for evaluating the microstructural environment of the brain.** *AJR Am J Roentgenol* 2014;202:W26–33. 10.2214/AJR.13.11365
10. Wakana S, Caprihan A, Panzenboeck MM, et al. **Reproducibility of quantitative tractography methods applied to cerebral white matter.** *Neuroimage* 2007;36:630–44. 10.1016/j.neuroimage.2007.02.049
11. Leclercq D, Duffau H, Delmaire C, et al. **Comparison of diffusion tensor imaging tractography of language tracts and**

intraoperative subcortical stimulations. *J Neurosurg* 2010; 112:503–11. 10.3171/2009.8.JNS09558
12. Hong JH, Choi BY, Chang CH, et al. **Injuries of the cingulum and fornix after rupture of an anterior communicating artery aneurysm: a diffusion tensor tractography study.** *Neurosurgery* 2012;70:819–23. 10.1227/NEU.0b013e3182367124
13. Kunimatsu A, Aoki S, Masutani Y, et al. **The optimal trackability threshold of fractional anisotropy for diffusion tensor tractography of the corticospinal tract.** *Magn Reson Med Sci* 2004;3:11–17. 10.2463/mrms.3.11
14. Oestreich LK, McCarthy-Jones S, Australian Schizophrenia Research Bank, et al. **Decreased integrity of the frontotemporal fibers of the left inferior occipito-frontal fasciculus associated with auditory verbal hallucinations in schizophrenia.** *Brain Imaging Behav* 2016;10:445–54. 10.1007/s11682-015-9421-5
15. Ashtari M, Cottone J, Ardekani BA, et al. **Disruption of white matter integrity in the inferior longitudinal fasciculus in adolescents with schizophrenia as revealed by fiber tractography.** *Arch Gen Psychiatry* 2007;64:1270–80. 10.1001/archpsyc.64.11.1270
16. Benjamin CF, Singh JM, Prabhu SP, et al. **Optimization of tractography of the optic radiations.** *Hum Brain Mapp* 2014; 35:683–97. 10.1002/hbm.22204
17. Kurki TJ, Laalo JP, Oksaranta OM. **Diffusion tensor tractography of the uncinate fasciculus: pitfalls in quantitative analysis due to traumatic volume changes.** *J Magn Reson Imaging* 2013;38:46–53. 10.1002/jmri.23901
18. Almasri O. ***An Essay on the Human Corticospinal Tract: History, Development, Anatomy, and Connections.*** *Neuroanatomy* 2011;10:1–4
19. Seo JP, Jang SH. **Different characteristics of the corticospinal tract according to the cerebral origin: DTI study.** *AJNR Am J Neuroradiol* 2013;34:1359–63. 10.3174/ajnr.A3389
20. Wycoco V, Shroff M, Sudhakar S, et al. **White matter anatomy: what the radiologist needs to know.** *Neuroimaging Clin N Am* 2013;23:197–216. 10.1016/j.nic.2012.12.002
21. Dum RP, Strick PL. **Frontal lobe inputs to the digit representations of the motor areas on the lateral surface of the hemisphere.** *J Neurosci* 2005;25:1375–86. 10.1523/JNEUROSCI.3902-04.2005
22. Lemon RN. **Descending pathways in motor control.** *Annu Rev Neurosci* 2008;31:195–218. 10.1146/annurev.neuro.31.060407.125547
23. Han BS, Hong JH, Hong C, et al. **Location of the corticospinal tract at the corona radiata in human brain.** *Brain Res* 2010;1326:75–80. 10.1016/j.brainres.2010.02.050
24. Holodny AI, Gor DM, Watts R, et al. **Diffusion-tensor MR tractography of somatotopic organization of corticospinal tracts in the internal capsule: initial anatomic results in contradistinction to prior reports.** *Radiology* 2005;234:649–53. 10.1148/radiol.2343032087
25. Kwon HG, Hong JH, Jang SH. **Anatomic location and somatotopic arrangement of the corticospinal tract at the cerebral peduncle in the human brain.** *AJNR Am J Neuroradiol* 2011; 32:2116–19. 10.3174/ajnr.A2660
26. Hong JH, Son SM, Jang SH. **Somatotopic location of corticospinal tract at pons in human brain: a diffusion tensor tractography study.** *Neuroimage* 2010;51:952–55. 10.1016/j.neuroimage.2010.02.063
27. Jang SH. **Somatotopic arrangement and location of the corticospinal tract in the brainstem of the human brain.** *Yonsei Med J* 2011;52:553–57. 10.3349/ymj.2011.52.4.553
28. Kwon HG, Hong JH, Lee MY, et al. **Somatotopic arrangement of the corticospinal tract at the medullary pyramid in the human brain.** *Eur Neurol* 2011;65:46–49. 10.1159/000323022
29. Lemon RN, Griffiths J. **Comparing the function of the corticospinal system in different species: organizational differences for motor specialization?** *Muscle Nerve* 2005;32:261–79. 10.1002/mus.20333
30. Rizzolatti G, Luppino G. **The cortical motor system.** *Neuron* 2001;31:889–901. 10.1016/S0896-6273(01)00423-8
31. Jang SH. **Perilesional reorganization of motor function in stroke patients.** *Neural Regen Res* 2010;5:1668–72
32. Catani M, Thiebaut de Schotten M. **A diffusion tensor imaging tractography atlas for virtual in vivo dissections.** *Cortex* 2008;44:1105–32. 10.1016/j.cortex.2008.05.004
33. Martino J, Brogna C, Robles SG, et al. **Anatomic dissection of the inferior fronto-occipital fasciculus revisited in the lights of brain stimulation data.** *Cortex* 2010;46:691–99. 10.1016/j.cortex.2009.07.015
34. Sarubbo S, De Benedictis A, Maldonado IL, et al. **Frontal terminations for the inferior fronto-occipital fascicle: anatomical dissection, DTI study and functional considerations on a multi-component bundle.** *Brain Struct Funct* 2013;218:21–37. 10.1007/s00429-011-0372-3
35. Duffau H, Herbet G, Moritz-Gasser S. **Toward a pluri-component, multimodal, and dynamic organization of the ventral semantic stream in humans: lessons from stimulation mapping in awake patients.** *Front Syst Neurosci* 2013;7:44
36. Martino J, Vergani F, Robles SG, et al. **New insights into the anatomic dissection of the temporal stem with special emphasis on the inferior fronto-occipital fasciculus: implications in surgical approach to left mesiotemporal and temporoinsular structures.** *Neurosurgery* 2010;66:4–12
37. Kljajevic V. **White matter architecture of the language network.** *Translational Neuroscience* 2014;5:239–52
38. Wu Y, Sun D, Wang Y, et al. **Subcomponents and connectivity of the inferior fronto-occipital fasciculus revealed by diffusion spectrum imaging fiber tracking.** *Front Neuroanat* 2016; 10:88
39. Hickok G, Poeppel D. **Towards a functional neuroanatomy of speech perception.** *Trends Cogn Sci* 2000;4:131–38. 10.1016/S1364-6613(00)01463-7
40. Hickok G, Poeppel D. **Dorsal and ventral streams: a framework for understanding aspects of the functional anatomy of language.** *Cognition* 2004;92:67–99. 10.1016/j.cognition.2003.10.011
41. Hickok G, Poeppel D. **The cortical organization of speech processing.** *Nat Rev Neurosci* 2007;8:393–402. 10.1038/nrn2113
42. Duffau H, Moritz-Gasser S, Mandonnet E. **A re-examination of neural basis of language processing: proposal of a dynamic hodotopical model from data provided by brain stimulation mapping during picture naming.** *Brain Lang* 2014;131:1–10. 10.1016/j.bandl.2013.05.011
43. Chang EF, Raygor KP, Berger MS. **Contemporary model of language organization: an overview for neurosurgeons.** *J Neurosurg* 2015;122:250–61. 10.3171/2014.10.JNS132647
44. ffytche DH, Blom JD, Catani M. **Disorders of visual perception.** *J Neurol Neurosurg Psychiatry* 2010;81:1280–87. 10.1136/jnnp.2008.171348

45. Kravitz DJ, Saleem KS, Baker CI, et al. **The ventral visual pathway: an expanded neural framework for the processing of object quality.** *Trends Cogn Sci* 2013;17:26–49. 10.1016/j.tics.2012.10.011
46. Ungerleider LG, Haxby JV. **'What' and 'where' in the human brain.** *Curr Opin Neurobiol* 1994;4:157–65. 10.1016/0959-4388(94)90066-3
47. van Polanen V, Davare M. **Interactions between dorsal and ventral streams for controlling skilled grasp.** *Neuropsychologia* 2015;79:186–91. 10.1016/j.neuropsychologia.2015.07.010
48. Doricchi F, Thiebaut de Schotten M, Tomaiuolo F, et al. **White matter (dis)connections and gray matter (dys)functions in visual neglect: gaining insights into the brain networks of spatial awareness.** *Cortex* 2008;44:983–95. 10.1016/j.cortex.2008.03.006
49. Epelbaum S, Pinel P, Gaillard R, et al. **Pure alexia as a disconnection syndrome: new diffusion imaging evidence for an old concept.** *Cortex* 2008;44:962–74. 10.1016/j.cortex.2008.05.003
50. ffytche DH, Catani M. **Beyond localization: from hodology to function.** *Philos Trans R Soc Lond B, Biol Sci* 2005;360:767–79. 10.1098/rstb.2005.1621
51. Fox CJ, Iaria G, Barton JJ. **Disconnection in prosopagnosia and face processing.** *Cortex* 2008;44:996–1009. 10.1016/j.cortex.2008.04.003
52. Catani M. **From hodology to function.** *Brain* 2007;130:602–05. 10.1093/brain/awm008
53. Forkel SJ, Thiebaut de Schotten M, Kawadler JM, et al. **The anatomy of fronto-occipital connections from early blunt dissections to contemporary tractography.** *Cortex* 2014;56:73–84. 10.1016/j.cortex.2012.09.005
54. Makris N, Kennedy DN, McInerney S, et al. **Segmentation of subcomponents within the superior longitudinal fascicle in humans: a quantitative, in vivo, DT-MRI study.** *Cereb Cortex* 2005;15:854–69. 10.1093/cercor/bhh186
55. Yagmurlu K, Middlebrooks EH, Tanriover N, et al. **Fiber tracts of the dorsal language stream in the human brain.** *J Neurosurg* 2016;124:1396–405. 10.3171/2015.5.JNS15455
56. Wang X, Pathak S, Stefaneanu L, et al. **Subcomponents and connectivity of the superior longitudinal fasciculus in the human brain.** *Brain Struct Funct* 2016;221:2075–92. 10.1007/s00429-015-1028-5
57. Catani M, Mesulam M. **The arcuate fasciculus and the disconnection theme in language and aphasia: history and current state.** *Cortex* 2008;44:953–61. 10.1016/j.cortex.2008.04.002
58. Thiebaut de Schotten M, Dell'Acqua F, Forkel SJ, et al. **A lateralized brain network for visuospatial attention.** *Nat Neurosci* 2011;14:1245–46. 10.1038/nn.2905
59. Rilling JK, Glasser MF, Preuss TM, et al. **The evolution of the arcuate fasciculus revealed with comparative DTI.** *Nat Neurosci* 2008;11:426–28. 10.1038/nn2072
60. Thiebaut de Schotten M, Dell'Acqua F, Valabregue R, et al. **Monkey to human comparative anatomy of the frontal lobe association tracts.** *Cortex* 2012;48:82–96. 10.1016/j.cortex.2011.10.001
61. Catani M, Thiebaut de Schotten M. *Atlas of Human Brain Connections*. Oxford: Oxford University Press; 2015
62. Chan-Seng E, Moritz-Gasser S, Duffau H. **Awake mapping for low-grade gliomas involving the left sagittal stratum: anatomofunctional and surgical considerations.** *J Neurosurg* 2014;120:1069–77. 10.3171/2014.1.JNS132015
63. Kinney HC, Brody BA, Kloman AS, et al. **Sequence of central nervous system myelination in human infancy. II. Patterns of myelination in autopsied infants.** *J Neuropathol Exp Neurol* 1988;47:217–34. 10.1097/00005072-198805000-00003
64. Dayan M, Munoz M, Jentschke S, et al. **Optic radiation structure and anatomy in the normally developing brain determined using diffusion MRI and tractography.** *Brain Struct Funct* 2015;220:291–306. 10.1007/s00429-013-0655-y
65. Piper RJ, Yoong MM, Kandasamy J, et al. **Application of diffusion tensor imaging and tractography of the optic radiation in anterior temporal lobe resection for epilepsy: a systematic review.** *Clin Neurol Neurosurg* 2014;124:59–65. 10.1016/j.clineuro.2014.06.013
66. Von Der Heide RJ, Skipper LM, Klobusicky E, et al. **Dissecting the uncinate fasciculus: disorders, controversies and a hypothesis.** *Brain* 2013;136:1692–707. 10.1093/brain/awt094
67. Levine B, Black SE, Cabeza R, et al. **Episodic memory and the self in a case of isolated retrograde amnesia.** *Brain* 1998;121(pt 10):1951–73. 10.1093/brain/121.10.1951
68. Fujie S, Namiki C, Nishi H, et al. **The role of the uncinate fasciculus in memory and emotional recognition in amnestic mild cognitive impairment.** *Dement Geriatr Cogn Disord* 2008;26:432–39. 10.1159/000165381
69. Yasmin H, Nakata Y, Aoki S, et al. **Diffusion abnormalities of the uncinate fasciculus in Alzheimer's disease: diffusion tensor tract-specific analysis using a new method to measure the core of the tract.** *Neuroradiology* 2008;50:293–99. 10.1007/s00234-007-0353-7
70. Agosta F, Henry RG, Migliaccio R, et al. **Language networks in semantic dementia.** *Brain* 2010;133:286–99. 10.1093/brain/awp233
71. Vigneau M, Beaucousin V, Hervé PY, et al. **Meta-analyzing left hemisphere language areas: phonology, semantics, and sentence processing.** *Neuroimage* 2006;30:1414–32. 10.1016/j.neuroimage.2005.11.002
72. Martino J, De Lucas EM. **Subcortical anatomy of the lateral association fascicles of the brain: a review.** *Clin Anat* 2014;27:563–69. 10.1002/ca.22321
73. Catani M, Jones DK, Donato R, et al. **Occipito-temporal connections in the human brain.** *Brain* 2003;126:2093–107. 10.1093/brain/awg203
74. Ashtari M. **Anatomy and functional role of the inferior longitudinal fasciculus: a search that has just begun.** *Dev Med Child Neurol* 2012;54:6–7. 10.1111/j.1469-8749.2011.04122.x
75. Martino J, De Witt Hamer PC, Vergani F, et al. **Cortex-sparing fiber dissection: an improved method for the study of white matter anatomy in the human brain.** *J Anat* 2011;219:531–41. 10.1111/j.1469-7580.2011.01414.x
76. Latini F. **New insights in the limbic modulation of visual inputs: the role of the inferior longitudinal fasciculus and the Li-Am bundle.** *Neurosurg Rev* 2015;38:179–89; discussion 189–90. 10.1007/s10143-014-0583-1
77. Ortibus E, Verhoeven J, Sunaert S, et al. **Integrity of the inferior longitudinal fasciculus and impaired object recognition in children: a diffusion tensor imaging study.** *Dev Med Child Neurol* 2012;54:38–43. 10.1111/j.1469-8749.2011.04147.x
78. Kleinhans NM, Richards T, Sterling L, et al. **Abnormal functional connectivity in autism spectrum disorders during face processing.** *Brain* 2008;131:1000–12. 10.1093/brain/awm334

79. Phillips OR, Nuechterlein KH, Clark KA, et al. **Fiber tractography reveals disruption of temporal lobe white matter tracts in schizophrenia.** *Schizophr Res* 2009;107:30–38. 10.1016/j.schres.2008.10.019
80. Pérez-Iglesias R, Tordesillas-Gutiérrez D, McGuire PK, et al. **White matter integrity and cognitive impairment in first-episode psychosis.** *Am J Psychiatry* 2010;167:451–58. 10.1176/appi.ajp.2009.09050716
81. Mandonnet E, Nouet A, Gatignol P, et al. **Does the left inferior longitudinal fasciculus play a role in language? A brain stimulation study.** *Brain* 2007;130:623–29. 10.1093/brain/awl361
82. Wu Y, Sun D, Wang Y, et al. **Segmentation of the cingulum bundle in the human brain: a new perspective based on DSI tractography and fiber dissection study.** *Front Neuroanat* 2016;10:84
83. Catheline G, Periot O, Amirault M, et al. **Distinctive alterations of the cingulum bundle during aging and Alzheimer's disease.** *Neurobiol Aging* 2010;31:1582–92. 10.1016/j.neurobiolaging.2008.08.012
84. Tuladhar AM, van Norden AG, de Laat KF, et al. **White matter integrity in small vessel disease is related to cognition.** *Neuroimage Clin* 2015;7:518–24. 10.1016/j.nicl.2015.02.003
85. Lin YC, Shih YC, Tseng WY, et al. **Cingulum correlates of cognitive functions in patients with mild cognitive impairment and early Alzheimer's disease: a diffusion spectrum imaging study.** *Brain Topogr* 2014;27:393–402. 10.1007/s10548-013-0346-2
86. Choo IH, Lee DY, Oh JS, et al. **Posterior cingulate cortex atrophy and regional cingulum disruption in mild cognitive impairment and Alzheimer's disease.** *Neurobiol Aging* 2010;31:772–79. 10.1016/j.neurobiolaging.2008.06.015
87. Sexton CE, Kalu UG, Filippini N, et al. **A meta-analysis of diffusion tensor imaging in mild cognitive impairment and Alzheimer's disease.** *Neurobiol Aging* 2011;32:2322.e5–18. 10.1016/j.neurobiolaging.2010.05.019